Relaxation of Bimolecular Layer Films on Water Surfaces

S. Kundu,*,† A. Datta,‡ and S. Hazra‡

Department of Materials Science, S.N. Bose National Centre for Basic Sciences, JD Block, Sector III, Salt Lake City, Kolkata 700 098, and Surface Physics Division, Saha Institute of Nuclear Physics, 1/AF Bidhannagar, Kolkata 700 064, India

Received February 29, 2008. Revised Manuscript Received June 2, 2008

Ferric stearate, a three-tailed amphiphile, forms bimolecular layers on water surfaces. Molecules in the lower layer are in an "asymmetric" configuration, Fe-containing heads touching water and three hydrocarbon tails in air, while molecules in the upper layer are in a "symmetric" configuration, in pairs of "Y and inverted Y" disposition of tails about the Fe-bearing head. Pressure relaxation at constant area ($\pi-t$ curves) and area relaxation at constant pressure ($A-t$ curves) of this bimolecular layer can be modeled as a sum of three exponential decay terms with distinct time constants and weight factors. Relating the long-term decay with desorption of the total film thus indicates a remarkable long-term stability of the bimolecular layer film. An X-ray reflectivity study of the bimolecular films deposited horizontally on Si(001) at various conditions of relaxation shows no further growth along the vertical of any other layer. Under pressure relaxation molecules are transferred from the upper layer to the lower layer with a change from symmetric to asymmetric configuration, while under area relaxation the transfer is from the lower layer to the upper layer with a configurational change from symmetric to asymmetric.

Introduction

Complex molecular systems constitute one of the most active and interdisciplinary fields of research, forming the link among mathematical, physical, and life sciences. However, what constitutes a "complex system" is probably difficult to specify. One effective way to label a molecular system as "complex" is to say that different parts of the system interact differently with the surroundings. Another way would be to choose a system with a hierarchy of structures at various length scales, while a third alternative is one with a hierarchy of motions at different time scales. Of course, it is intuitively or qualitatively apparent that these alternative definitions are interrelated, but a quantitative relation between, say, structural and dynamical hierarchies is, in fact, the central issue in the understanding of complex systems. It would indeed be useful, in this connection, to have a molecular system that has complex dynamics but a not too complex structure, i.e., with a small number of distinct structural components, which, on the other hand, exert completely different kinds of forces on the surroundings.

Molecular layers of amphiphiles, i.e., molecules with hydrophilic and hydrophobic moieties, at the air−water interface are known as Langmuir monolayers.[1–5] Such layers furnish good examples of the "tractable" complex molecular systems discussed above. Even the structurally simpler amphiphiles, consisting of a polar group such as OH (alcohol), NH_2 (amine), COOH (carboxylic acid), COOM (salt; M = metal), or COOR (ester; R = alkane) and a nonpolar group such as a hydrocarbon with more than 12 carbon atoms, show complex dynamics at the air−water interface.

There are two different processes by which these complex temporal behaviors have been investigated. One is called "area relaxation", where the surface pressure of the film is kept at a fixed target pressure as the barrier moves with time. The other is "pressure relaxation", where the barrier is kept fixed after the target pressure is reached and the surface pressure of the film decreases with time. After the target pressure is reached, the film reorganizes spontaneously to obtain the state of lower Gibbs energy at a lower surface pressure or area. This decrease of surface pressure or area with time is the relaxation curve of the film, and it gives information about the mechanism behind film relaxations.[6,7] There are different proposed models of relaxations, where different algebraic and exponential decays have been considered. In the model proposed by Vollhardt et al.,[8,9] the area relaxations were described by a "nucleation and growth" theory where 2D to 3D nucleations have been considered. Using Brewster angle microscopy (BAM), the corresponding condensed phases have been visualized at the air−water interface.[10,11] In this way relaxations of fatty acids and fatty amines and their mixtures have been studied by BAM on the water surface.[12] By transferring such relaxed films onto some solid substrate and then using atomic force microscopy (AFM), the corresponding morphology and relaxation behavior have been verified.[13] In some cases the relaxation of the Langmuir monolayer is expressed as a sum of three exponentials,[14] where the two shorter decay constants (a few minutes and tens of minutes) of the exponential decay were due to the short- and long-range monolayer reorganization and the third, longer (hundreds to thousands of minutes) decay constant was for monolayer desorption in the subphase.

* To whom correspondence should be addressed. E-mail: sarathi@bose.res.in or sarathi.kundu@gmail.com.

† S.N. Bose National Centre for Basic Sciences.

‡ Saha Institute of Nuclear Physics.

(1) Gaines, G. L. *Insoluble Monolayers at Liquid-Gas Interfaces*; Interscience: New York, 1966.

(2) Kaganer, V. M.; Möhwald, H.; Dutta, P. *Rev. Mod. Phys.* **1999**, *71*, 779.

(3) Gourier, C.; Daillant, J.; Braslau, A.; Alba, M.; Quinn, K.; Luzet, D.; Blot, C.; Chatenay, D.; Grübel, G.; Legrand, J.-F.; Vignaud, G. *Phys. Rev. Lett.* **1997**, *78*, 3157.

(4) Kmetko, J.; Datta, A.; Evmenenko, G.; Dutta, P. *J. Phys. Chem. B* **2001**, *105*, 10818.

(5) Ries, H. E., Jr *Nature* **1979**, *281*, 287.

(6) Vollhardt, D. *Colloids Surf., A* **1998**, *143*, 185.

(7) Vollhardt, D. *Colloids Surf., A* **1999**, *156*, 79.

(8) Vollhardt, D.; Retter, U. *J. Phys. Chem.* **1991**, *95*, 3723.

(9) Vollhardt, D.; Retter, U.; Seigel, S. *Thin Solid Films* **1991**, *199*, 189.

(10) Angelova, A.; Vollhardt, D.; Ionov, R. *J. Phys. Chem.* **1996**, *100*, 10710.

(11) Vollhardt, D.; Gutberlet, T. *Colloids Surf., A* **1995**, *102*, 257.

(12) Lee, Y.-L.; Liu, K.-L. *Langmuir* **2004**, *20*, 3180.

(13) Vollhardt, D.; Kato, T.; Kawano, M. *J. Phys. Chem.* **1996**, *100*, 4141.

(14) Viseu, M. I.; Goncalves da Silva, A. M.; Costa, S. M. B. *Langmuir* **2001**, *17*, 1529.

10.1021/la8006487 CCC: $40.75
Published on Web 07/30/2008

A convenient and systematic way to increase the structural complexity of these amphiphiles is to increase either the number of headgroups or the number of tails. Increasing the number of hydrocarbon chains or tails can be done by preparing salts of amphiphilic fatty acids with multivalent metals. Indeed, preformed, three-tailed amphiphilic salts, such as ferric stearate [FeSt, $(CH_3(CH_2)_{18}COO)_3Fe$], are found to form a bimolecular film on the water surface,[15] instead of a Langmuir monolayer. In this bimolecular film the molecules in the bottom layer are in the typical "asymmetric" configuration, with all the heads touching water and all three tails on the same side of the Fe-bearing headgroups, i.e., up in the air, whereas molecules in the upper layer form pairs in the "Y and inverted Y" configuration[16] where the tails in each pair are in an overall "symmetric" configuration about the Fe-bearing headgroups. This bimolecular film[15,17] reduces the surface tension of water by almost 2 orders of magnitude[15] and is quite different from the usual Langmuir monolayer in its response to mechanical stress such as compression. It was also shown that horizontal transfer[15,17] of the bimolecular film onto substrates from the water surface does not make any remarkable changes either in the out-of-plane structure or in the in-plane morphology.

For this complex bimolecular film with different molecular configurations in its two layers, relaxation studies are important to see the temporal behavior of the overall film and also of the two individual molecular layers forming the film. The distinct structures of the molecules in the two layers of this bimolecular film allow us, through X-ray reflectivity, to observe the details of these relaxation mechanisms. In this study, we have addressed these points through the fitting of $\pi-t$ (surface pressure $\pi = \gamma_0 - \gamma$, $\gamma_0(\gamma)$ being the surface tension of (film-covered) water and t = time) curves in pressure relaxation and $A-t$ (A = specific molecular area = area occupied per molecule on the water surface) curves in area relaxation and by X-ray reflectivity analysis of films transferred onto Si(001) substrates using the modified inverted Langmuir−Schaefer (MILS) method of horizontal film transfer.

Experimental Details and Reflectivity Technique

The preparation and purification process of FeSt has been described elsewhere.[15,16] First, sodium stearate was prepared by adding sodium hydroxide (Merck, 99%) to hot Milli-Q water (resistivity 18.2 MΩ cm) containing stearic acid (Sigma, 99.8%) in appropriate amounts. Sodium hydroxide was added until the medium was slightly alkaline (pH ≈ 7.0−7.5). Sodium stearate is completely soluble in hot water. Measured amount of ferric chloride (Merck, 99%) solution was then added to the freshly prepared sodium stearate solution in hot conditions so FeSt was formed, which was collected after filtration. As FeSt is completely insoluble in water at all temperatures, it was then washed repeatedly by hot Milli-Q water to remove unreacted sodium stearate and other water-soluble impurities. It was then washed with benzene (SLR, 99.8%) to remove unreacted stearic acid and other organic impurities. FeSt molecules were spread from 250 μL of a 0.6 mg/mL chloroform (Aldrich, 99.98%) solution onto Milli-Q water in a Langmuir trough (KSV 5000) at 24 °C. The pH of the subphase water was ∼5.5 at the time of isotherm measurement and film depositions. A platinum Wilhelmy plate was used to measure the surface pressure of the FeSt film. The films were compressed with two different barrier speeds, 10 mm/min (slow) and 70 mm/min (fast). For each kind of barrier speed, three different target pressures (π_T), i.e., 15, 30, and 50 mN/m, were used for area and pressure relaxation measurements.

Deposition of the FeSt films by the MILS method has been described previously.[15,17] Hydrophilic silicon substrate was kept horizontally in a homemade L-shaped Teflon substrate holder, which was attached to the clip of the trough dipper and immersed into the water. FeSt molecules were spread on the water surface from the same solution (0.6 mg/mL) with the same amount as was spread at the time of all relaxation measurements. Silicon substrates were made hydrophilic by keeping them in a solution of ammonium hydroxide (NH_4OH; Merck, 98%), hydrogen peroxide (H_2O_2; Merck, 98%), and Milli-Q water (water:NH_4OH:H_2O_2 = 2:1:1 by volume) for 5−10 min at 100 °C. Depositions were done after a fixed target pressure (30 mN/m) was reached and for three different conditions: (a) immediately after the target pressure (type 1) was reached, (b) after area relaxation for 2 h (type 2), and (c) after pressure relaxation for 2 h (type 3). All three types of depositions were made for the two above-mentioned compression speeds at 24 °C. For each relaxation measurement and film deposition fresh Milli-Q water was used in the trough. The upward speed of the substrate holder was 0.5 mm/min for all depositions to cause minimum disturbance.

Reflectivity studies of all deposited FeSt films were carried out using an X-ray diffractometer (D8 Discover, Bruker AXS) with a Cu source (sealed tube) followed by a Göbel mirror to select and enhance Cu Kα radiation (λ = 1.54 Å). The diffractometer has a 2-circle goniometer [$\theta(\omega)-2\theta$] with a 1/4-circle Eulerian cradle as the sample stage. The cradle has two rotational (χ and ϕ) and three translational (X, Y, and Z) motions. The scattered beam was detected using a NaI scintillation (point) detector. Measurements were done for $\phi = 0°$, $\chi = 0°$, and varying θ and 2θ in steps of millidegrees. Instrumental resolution in the out-of-plane direction was 0.0014 $Å^{-1}$. The scattering plane is perpendicular to the sample face. Data were taken in the specular condition; i.e., the incident angle was equal to the exit angle, and both were in the scattering plane. Under specular conditions the momentum transfer vector $q = k_f - k_i$ ($k_{i(f)}$ = incident (scattered) wave vector) has only one nonvanishing component, q_z, normal to the surface and given by $q_z = (4\pi/\lambda)\sin\theta$, where θ is the angle the incident X-ray beam makes with the surface.[18−20] The data collection time for a single sample was about 50 min, and reflectivity data for all the samples were collected approximately after two days of sample preparation. Proper footprint correction and normalization of all the specular reflectivity curves were made considering the sample size, incident beam width, and maximum value of the reflectivity data.[20]

The refractive index (n) of a material for X-rays can be described by $n = 1 - \delta - i\beta$, where δ and β represent the scattering strength and the absorption of the material, respectively. For X-rays, $\delta = r_0\rho_{el}\lambda^2/2\pi$ and $\beta = \mu\lambda/4\pi$, where λ is the X-ray wavelength, ρ_{el} is the electron density, r_0 is the classical electron radius (2.82×10^{-5} Å), and μ is the linear absorption coefficient. Depending on the different electron densities (ρ_{el}) of the materials along the surface normal (z), variation in the specular reflectivity profile was obtained. X-ray reflectivity data of all the deposited films were analyzed by the Parratt formalism,[19,20] introducing finite interfacial widths.[21,22] The interfacial width behaved as a Debye−Waller-like factor and reduced the reflected intensity. An instrumental resolution in the form of a Gaussian function and a constant background were also included at the time of data analysis. For the analysis, one needs a reasonable model as an input that minimizes the deviation between the experimental data and the calculated reflectivity profiles based on a fitting program. Analysis of the X-ray reflectivity data of all the deposited films gives electron density profiles (EDPs), i.e., distribution of ρ_{el} along z, from which the out-of-plane structural information, i.e., total film thickness, individual layer thickness, interfacial roughness, electron densities of the individual layers, etc., are extracted. Thus, comparative out-of-plane structural studies

(15) Datta, A.; Kundu, S.; Sanyal, M. K.; Daillant, J.; Luzet, D.; Blot, C.; Struth, B. *Phys. Rev. E* **2005**, *71*, 041604.
(16) Datta, A.; Sanyal, M. K.; Dhanabalan, A.; Major, S. S. *J. Phys. Chem. B* **1997**, *101*, 9280.
(17) Kundu, S.; Datta, A.; Hazra, S. *Langmuir* **2005**, *21*, 5894.
(18) Basu, J. K.; Hazra, S.; Sanyal, M. K. *Phys. Rev. Lett.* **1999**, *82*, 4675.
(19) Parratt, L. G. *Phys. Rev.* **1954**, *95*, 359.
(20) Basu, J. K.; Sanyal, M. K. *Phys. Rep.* **2002**, *363*, 1.
(21) Daillant, J.; Gibaud, A. *X-Ray and Neutron Reflectivity: Principles and Applications*; Springer: Berlin, 1999.
(22) Tolan, M. *X-Ray Scattering from Soft Matter Thin Films*; Springer: Berlin, 1999.

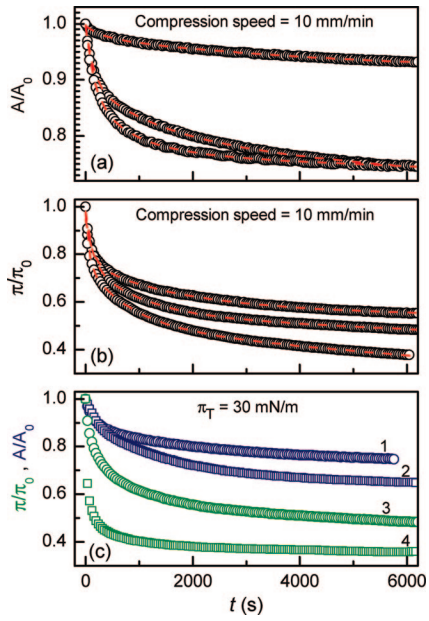

Figure 1. (a) Normalized $A-t$ curves in area relaxation at constant pressure. The three curves (shown by open circles) are for three different target pressures, i.e., for $\pi_T = 15$, 30, and 50 mN/m, respectively, from top to bottom. The solid lines are the corresponding fits by the relaxation model (see the text). (b) Normalized $\pi-t$ curves in pressure relaxation at constant area. The three curves (shown by open circles) are for three different target pressures, i.e., for $\pi_T = 15$, 30, and 50 mN/m, respectively, from top to bottom. The solid lines are the corresponding fits by the relaxation model (see the text). (c) Normalized $A-t$ (1 and 2) and $\pi-t$ (3 and 4) curves for a fixed target pressure $\pi_T = 30$ mN/m and for two different barrier speeds, slow (10 mm/min, 1 and 3) and fast (70 mm/min, 2 and 4).

Table 1. Weight Factors (a_i) and Time Constants (τ_i) Obtained by Fitting the $A-t$ Decay Curves to a Three-Exponential Model (Eq 1) for Slow and Fast Barrier Speeds

π_T (mN/m)	speed (mm/min)	a_1	τ_1 (10^2 s)	a_2	τ_2 (10^3 s)	a_3	τ_3 (10^5 s)
15	10	0.01	1.29	0.03	1.26	0.96	2.06
30	10	0.10	1.47	0.11	1.51	0.78	1.13
50	10	0.12	1.69	0.11	0.84	0.77	1.98
15	70	0.02	1.89	0.03	3.28	0.95	7.41
30	70	0.09	1.55	0.23	1.30	0.69	1.05
50	70	0.07	1.62	0.27	0.45	0.66	4.64

of these three types of deposited samples (type 1, type 2, and type 3) can be made from the reflectivity analysis.

Isotherm Studies

Area Relaxation. In Figure 1a area relaxations of the FeSt films are shown for three different target pressures (15, 30, and 50 mN/m) and for a slow barrier speed, i.e., for 10 mm/min. It is clear that with increasing target pressure the area of the FeSt film drops rapidly initially and slowly in the later stages. All the relaxation curves can be fitted with an exponential decay model comprising a combination of three decay terms:

$$A/A_0 = a_1 \exp(-t/\tau_1) + a_2 \exp(-t/\tau_2) + a_3 \exp(-t/\tau_3) \quad (1)$$

where a_i are three different weight factors and τ_i are three different time constants.

Relaxation curves were also taken for those three target pressures at a fast barrier speed (70 mm/min). The corresponding weight factors and time constants for area relaxations are shown in Table 1. It has also been observed that for the same target pressure the FeSt film relaxes more rapidly with increasing barrier compression speed as shown in Figure 1c for the 30 mN/m target pressure. It is seen from the values of Table 1 that the initial time constants, i.e., τ_1 and τ_2, are on the order of 10^2 and 10^3 s, respectively, while the third, i.e., τ_3, is on the order of 10^5 s. The corresponding weight factors for the initial two exponentials are small values, while the third is large. This implies that the first two decay processes exist for small times with small contributions while the third decay process exists for a long time with a large contribution. The weight factors a_1 and a_2 are very small for the lowest target pressure (15 mN/m) and increase for higher target pressures and remain nearly constant, while the third weight factor, a_3, decreases with increasing target pressure. This implies that with increasing target pressure the contribution of the first two decay processes becomes saturated but that of the third decreases, indicating the dependence on the initial target pressure.

Table 2. Weight Factors (a_i') and Time Constants (τ_i') Obtained by Fitting the $\pi-t$ Decay Curves to a Three-Exponential Model (Eq 2) for Slow and Fast Barrier Speeds

π_T (mN/m)	speed (mm/min)	a_1'	τ_1' (10^2 s)	a_2'	τ_2' (10^3 s)	a_3'	τ_3' (10^5 s)
15	10	0.18	1.27	0.19	1.61	0.58	1.20
30	10	0.21	1.27	0.22	0.99	0.55	0.50
50	10	0.21	0.65	0.26	0.83	0.50	0.21
15	70	0.24	0.59	0.17	0.86	0.53	0.34
30	70	0.38	0.32	0.16	0.40	0.39	0.61
50	70	0.53	0.14	0.17	0.23	0.28	0.25

Pressure Relaxation. In Figure 1b pressure relaxations of the FeSt films are shown for 15, 30, and 50 mN/m target pressures and for a slow barrier speed. Like area relaxations the pressure of the FeSt film drops rapidly initially and slowly over a longer time. This behavior is enhanced with increasing target pressure. It has also been observed that, like area relaxation, for the same target pressure the FeSt film relaxes more rapidly for increased barrier compression speed as shown in Figure 1c for the 30 mN/m target pressure. All the relaxation curves are fit with a combination of three exponential decay terms:

$$\pi/\pi_0 = a_1' \exp(-t/\tau_1') + a_2' \exp(-t/\tau_2') + a_3' \exp(-t/\tau_3') \quad (2)$$

where a_i' are three different weight factors and τ_i' are three different time constants.

The corresponding weight factors and time constants for pressure relaxations with low and high barrier speeds are shown in Table 2. It is seen from Table 2 that the initial time constants, i.e., τ_1' and τ_2', are on the order of 10^2 and 10^3 s, respectively, while the third, i.e., τ_3', is on the order of 10^5 s. The corresponding weight factors for the initial two exponentials are small values compared with the third, which is large. The weight factors a_1' and a_2' on the average increase from lower values to higher values with increasing target pressure, while the third weight factor, a_3', decreases with increasing target pressures. Nearly the same types of features are also observed for area relaxations.

Comparison with Monolayer and Combined Systems. It is clear that with increasing target pressure, the pressure and the area of the FeSt film drop. The main characteristics are that the area and pressure losses are rapid in the initial relaxation stage and then are very slow at longer time scales. It has also been observed that the film relaxes more rapidly with increasing barrier compression speed. These types of features have also been observed in the mixture of anionic and cationic monolayers[14] at the air−water interface. Like this mixing system, the stability of this FeSt film is also very large. Also the time constants and the weight factors of the three decay terms in that "catanionic" mixture are quite similar in value to the three decays terms of

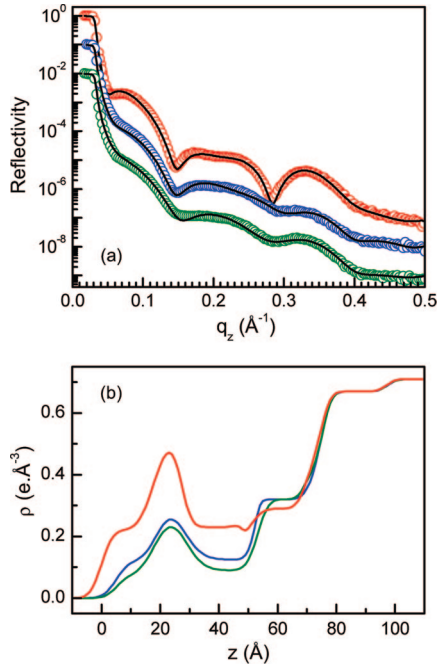

Figure 2. (a) Normalized reflectivity (open circles) and corresponding fit (solid line) for the films deposited by the MILS method. The top profile is for a film of type 2, the middle one is for a type 1 film, and the bottom profile is for a film of type 3 (see the text). (b) Corresponding EDPs shown in the same order from top to bottom. Air is at $z = 0$. All films were deposited with a slow (10 mm/min) barrier speed.

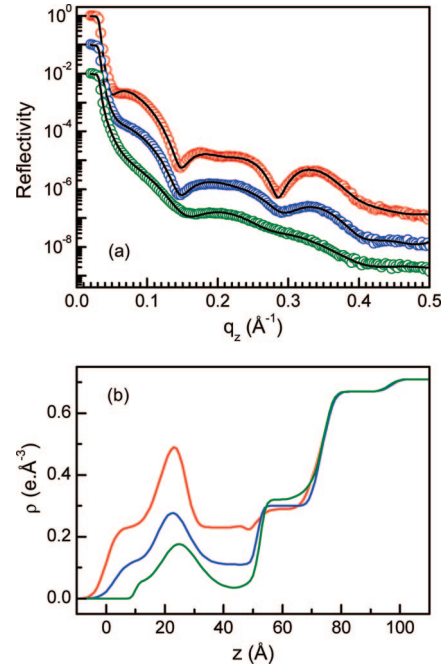

Figure 3. (a) Normalized reflectivity (open circles) and corresponding fit (solid line) for the films deposited by the MILS method. The top profile is for a film of type 2, the middle one is for a type 1 film, and the bottom profile is for a film of type 3 (see the text). (b) Corresponding EDPs shown in the same order from top to bottom. Air is at $z = 0$. All films were deposited with a fast (70 mm/min) barrier speed.

our bimolecular systems. The major difference is in the pressure relaxation where the long-term decay has less weight in comparison to the short-term decay. The same type of more stable monolayer has also been observed for a stearic acid and octadecylamine (ODA) mixture,[12] where with increasing ODA amount the overall stability of the film increases. Contrary to the area relaxation of normal fatty acid monolayers, all $A-t$ curves for area relaxation are not fit by a single exponential decay,[8,12] e.g., the model proposed by Vollhardt et al.[8,9] where relaxation mechanisms are proposed due to the formation of progressive nucleation and hemispherical growth.

X-ray Reflectivity of Bimolecular Films: Reflectivity Results

In Figure 2a, we show normalized reflectivity profiles of films for which a slow barrier speed was used, while in Figure 3a these are shown for films with a fast barrier speed. In both figures, the top profile is for a film of type 2, where 2 h of area relaxation was allowed before film deposition after the target pressure of 30 mN/m was reached. The middle profile is obtained from a film of type 1, which was deposited just after the target pressure was reached. The film deposition conditions for the bottom profile are the same as those of the top one, but the only difference is that it was deposited after 2 h of pressure relaxation. This is a film of type 3. X-ray reflectivity data of all the deposited films were analyzed by the Parratt formalism,[19,20] introducing finite interfacial widths[21,22] as described before. EDPs obtained from the fits of the reflectivity data are also shown in the same order (from top to bottom). All EDPs corresponding to Figure 2a are shown in Figure 2b, while EDPs corresponding to Figure 3a are shown in Figure 3b.

The two-molecular-layer model[15,17] of Figure 4 fits all reflectivity profiles. In the lower molecular layer, all three hydrophobic tails of the FeSt molecules are on one side and the hydrophilic head is on the other side. In this configuration

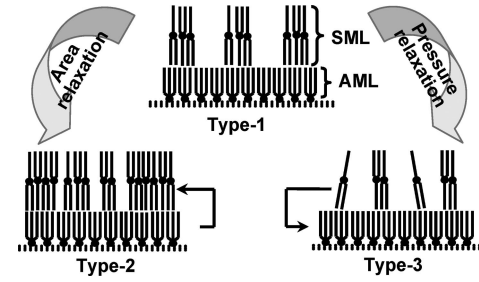

Figure 4. Schematic of the molecular arrangement before (type 1) and after area (type 2) and pressure (type 3) relaxations. In the area relaxation mechanism asymmetric molecules from the AML move to the SML, changing the configuration to symmetric. In the pressure relaxation mechanism symmetric molecules from the SML move to the AML, changing the configuration to asymmetric.

the molecules have an amphiphilic nature and can make a stable monolayer on the water surface. We call this monolayer the "asymmetric monolayer", or AML. In the upper molecular layer, FeSt molecules have the configuration where the head is in the middle and the two tails are on two sides. We call this the symmetric configuration and this stable monolayer of molecules in the symmetric configuration: the "symmetric monolayer", or SML. Of course, the thickness of the SML is twice that of the AML, and thus, the thickness of the bimolecular layer is 3 times that of the AML. In the SML, the configuration of the molecules has a hydrophobic nature and is unstable on the water surface but can make a stable monolayer on a hydrocarbon surface such as oil, a hydrophobic substrate,[23] or an AML.

The most remarkable result obtained from the EDPs is that, at the observed points in the relaxation curves, we could not see any growth above this bimolecular layer. Spontaneous growth

(23) Mukhopadhyay, M. K.; Sanyal, M. K.; Datta, A.; Webster, J.; Penfold, J. *Chem. Phys. Lett.* **2005**, *407*, 276.

to multilayers is completely inhibited during either pressure or area relaxation. This indicates an unusually high stability of the bimolecular layer structure, and existing models of Langmuir monolayer relaxation such as the 2D−3D transition paradigm of Vollhardt are not applicable. We now proceed to probe into the microscopic dynamics of relaxation of this bimolecular layer structure to understand the basis of its stability.

From Figure 2b it is seen that, during area relaxation, the SML density of the upper EDP increases in comparison to the SML density of the middle EDP. Hence, it can be argued that, as the barrier moves to maintain the fixed pressure during area relaxation, the asymmetric molecules from the AML move to the SML in a symmetric configuration. On the other hand, for pressure relaxation, where the barrier is fixed, the SML density decreases as seen from the lower EDP. For all the films, the AML density remains nearly the same and compact as observed from the EDPs. Integrating the obtained EDPs, we get the number of electrons per square angstrom. The calculated number of electrons of the FeSt molecule in the AML configuration is 8.39 electrons/Å^2, considering 20 Å^2 to be the cross-sectional area occupied by each hydrocarbon chain at 100% film coverage. From this we can obtain the different coverages of the AMLs and SMLs of the deposited films, keeping in mind that for the same coverage the number of molecules in the SML configuration is twice the number in the AML configuration. Thus, for a slow barrier speed, the AML and SML coverages in the film deposited just after the target pressure is reached (type 1) are 95% and 36%, respectively. The corresponding AML and SML coverages for area relaxation (type 2) are 92% and 74%, and for pressure relaxation (type 3) they are 92% and 29%, respectively. For a high barrier speed, the AML and SML coverages in type 1 films are 91% and 39%, whereas the corresponding coverages for area relaxation (type 2) are 100% and 74% and those for pressure relaxation (type 3) are 88% and 19%, respectively. It can be noted that all the coverages obtained from the EDPs can have a maximum error of about 6%.

It is to be mentioned that, even with the low coverage on the top layer, we do not see any tilt of the tails. This is, however, consistent with the earlier results,[15] where FeSt bimolecular layers, either on water or on substrates, are seen to remain untilted even at very low coverage, possibly due to the larger tail−tail interaction caused by the larger number of tails per molecule.

Relaxation Model

All the $\pi-t$ curves in pressure relaxation and $A-t$ curves in area relaxation are strongly dependent on the target pressure and barrier speed. According to the previous literature,[14,24] two types of reorganization as indicated by the first two exponential terms of the relaxation model, which are on short time scales ($\sim 10^2$ and 10^3 s), are assumed due to two mechanisms. We have, a priori, followed this line of thought and have also assigned these decay terms to similar mechanisms. While the first was assumed to be due to a local, short-range reorganization of the headgroups and tails of the constituent molecules, the second reorganization was proposed to be due to a long-range rearrangement of the molecules in the bimolecular film. In the conventional Langmuir monolayers, either mixed or pure, the third decay term in this model is assigned to global material loss or desorption.[25] However, for our complex bimolecular layer, we refrain from attaching any specific physical significance to the long-term decay. Isotherm experiments result in bimolecular layer films having nearly the same kind of behavior for area and pressure relaxations, but the reflectivity profiles of the deposited films give more quantitative distinctions between these processes in terms of the electrons or molecules lost and gained due to different kinds of relaxations.

Thus, from the analysis of the EDPs we obtain a precise, molecular mechanism of the relaxation processes of this bimolecular layer. It is seen quantitatively that the SML density increases considerably with area relaxations, which implies conversion from an asymmetric to a symmetric molecular configuration of these three-tailed amphiphiles. As the barrier moves, molecules go from the AML to the SML, and on average ∼38% (for low and high speeds) of the SML coverage increases compared to the SML coverage of the type 1 film. The corresponding changes in AML coverage are ∼2% (slow) and ∼9% (fast). On the other hand, in pressure relaxation, the EDPs show that, although the SML coverage decreases on average ∼7% (slow) and ∼20% (fast), the AML coverage decreases by ∼3% for both low and high speeds; i.e., it remains nearly unchanged. This is possible only if molecules in the SML come down to the AML in pressure relaxations as vacancies are generated in the lower layer. We suggest tentatively that the interconversion between the symmetric and asymmetric configurations is the "molecular rearrangement" involved in the first decay term, while the transfer of molecules from the upper layer to the lower layer and vice versa constitutes the "rearrangement" that represents the second decay term. These are shown in cartoon form for area relaxation and pressure relaxation in Figure 4. For area relaxation, the film goes from type 1 to type 2, whereas for pressure relaxation it goes from type 1 to type 3. In both relaxations, the bimolecular layer structure is maintained (where the upper SML is "gaslike" in positional order[26]). Only the number of molecules in the SML changes, keeping the number of molecules in the AML nearly constant. For area relaxation the number of molecules, i.e., coverage, in the SML increases due to the conversion of molecules from an asymmetric to a symmetric configuration, whereas for pressure relaxation the reverse occurs. Only at very low coverage in the SML the molecules can tilt, which can decrease the SML layer thickness by a small amount.

We add that, as these X-ray data were taken on films transferred onto substrates and not onto a water surface, there might be an extra relaxation term due to the difference in interaction between the AML and water and the AML and substrate. However, as we pointed out earlier, the deviations in structure and structural correlations are small for FeSt films through MILS, but they cannot be totally discounted. In addition, we make it clear that, from our X-ray reflectivity analysis, we have obtained the out-of-plane structural information of the film after 2 h of area and pressure relaxations and have compared that with the structure of the film deposited immediately after the target pressure was reached. Hence, we cannot separate out any kind of structural modifications due to short-term relaxations (i.e., for which τ is $\sim 10^2$ and $\sim 10^3$ s). This does not depend on the data collection time or on whether some other relaxation, involving a very long τ, is occurring on the solid substrate or not. All we obtain is the structural modifications after these short-term relaxations together with long-term relaxations and their variation with different types of relaxations.

The major observations on the temporal behavior of the bimolecular film as a whole are (i) similar to a Langmuir monolayer, the bimolecular layer also has three distinct time

(24) Gupta, S. K.; Taylor, D. M.; Dynarowicz, P.; Barlow, E.; Wainwright, C. E. A.; Underhill, A. E. *Langmuir* **1992**, *8*, 3057.

(25) Albrecht, O.; Matsuda, H.; Eguchi, K.; Nakagiri, T. *Thin Solid Films* **1999**, *338*, 252.

(26) Kundu, S.; Datta, A.; Sanyal, M. K.; Daillant, J.; Luzet, D.; Blot, C.; Struth, B. *Phys. Rev. E* **2006**, *73*, 061602.

scales of relaxation, τ_1 ($\sim 10^2$ s), τ_2 ($\sim 10^3$ s), and τ_3 ($\sim 10^5$ s), corresponding perhaps to molecule-level, domain-level, and film-level readjustments and (ii) the bimolecular layer is more stable than the typical Langmuir monolayer and, in this aspect, resembles binary mixed monolayers, i.e., Langmuir monolayers with horizontal mixing.

The second point is interesting as it indicates energy transfer between the two molecular species in both cases. As our X-ray scattering studies show, in the bimolecular layer this probably takes place through the interconversion of molecules between the two layers. This exchange has to be accompanied by configurational changes that correspond to the energy minima at and away from the water surface: while the AML is preferred strongly at the water surface, the SML only is allowed away from it. It is also remarkable that while in area relaxation the transfer is from the AML to the SML, in pressure relaxation it is from the SML to the AML. In the former, energy is supplied by pushing the barrier, i.e., externally, and hence there is actually an internal resistance to the AML to SML conversion. On the other hand, when the system is left alone, pressure relaxation takes place, where the SML to AML conversion occurs. This means that the inherent tendency of the bimolecular layer is to maintain molecules in the AML or, in other words, at the water surface. A possible reason behind this tendency or "driving force" can be the dipolar interaction between water and FeSt molecules in the AML, since the molecules have a considerable dipole moment only in this configuration. An interesting extension of these studies would be to compare relaxation processes of such bimolecular layers during compression and expansion or more precisely measurements for AML to SML conversion vis-à-vis for SML to AML conversion to measure the hysteresis and to understand whether these changes in molecular configurations play any specific roles in this hysteresis.

Conclusions

Increasing the structural complexity of an amphiphile by the "incremental step" of increasing the number of tails to three, in ferric stearate, we obtain a bimolecular layer on water surface instead of a monomolecular Langmuir monolayer as obtained with single-tailed amphiphiles. In this bimolecular layer, the molecules in the lower layer are in the asymmetric configuration with respect to the metal-bearing headgroups where all hydrocarbon tails are on one side of the headgroups and in the upper molecular layer the molecules are in the symmetric configuration where the tails are on both sides of the headgroups, making Y and inverted Y structures. Here we have presented some results of the studies on the temporal behavior of this bimolecular layer. Specifically, we have investigated the area and pressure relaxations of these films from surface-pressure-specific molecular area isotherms. We have looked at the molecular mechanisms involved in these relaxation processes from X-ray reflectivity measurements on films horizontally transferred onto Si substrates under different relaxation conditions.

We have found that, like Langmuir monolayers and, in particular, like mixed Langmuir monolayers of cationic and anionic surfactants, the bimolecular layer has three exponential decay terms in its area and pressure relaxation curves: a probable short-range molecular rearrangement (time constant $\tau \approx 10^2$ s), a longer range rearrangement ($\tau \approx 10^3$ s), and a film-level relaxation ($\tau \approx 10^5$ s). The weight factors of these decay terms also match the corresponding terms in mixed Langmuir monolayers in their values, except in the case of pressure relaxation where the long-term loss becomes less important and molecular rearrangements become more important in the bimolecular layer as compared to the mixed monolayer, showing that the bimolecular layer is more stable at least for pressure relaxation. We have also found that, unlike Langmuir monolayers, relaxation in the bimolecular layer does not lead to any further vertical growth, i.e., addition of more layers. As for the molecular mechanism of rearrangements, we have found that conversions from asymmetric to symmetric molecular configurations in area relaxations and from symmetric to asymmetric molecular configurations in pressure relaxations are taking place, keeping the bimolecular layer structure unchanged on the water surface.

LA8006487